Surface properties of sol–gel-based fluorine-containing ceramic coatings

Mustafa Hulusi Uğur[1] · Emrah Çakmakçı[1] · Atilla Güngör[1] · Nilhan Kayaman-Apohan[1]

Abstract

In this work, sol–gel-based non-stick ceramic coating formulations were prepared and coated onto aluminum panels in order to investigate their surface properties. The effect of the addition of optimal amount of fluorine-containing silane compound (FAS) on the surface and adhesion properties were also investigated. The morphology, structure, and elemental chemical composition of the coatings were characterized by scanning electron microscopy, atomic force microscopy (AFM), energy dispersion spectrum (SEM/EDAX), Fourier-transform infrared spectroscopy (FTIR), and X-ray photoelectron spectroscopy (XPS), respectively. Moreover, several properties of the coatings such as cross-cut adhesion, hardness, gloss, and contact angle (CA) were determined. When fluorine was introduced, the pencil hardness was increased to 6H. Fluorinated non-stick ceramic coatings were found to have good adhesion on the aluminum substrates.

Graphical Abstract
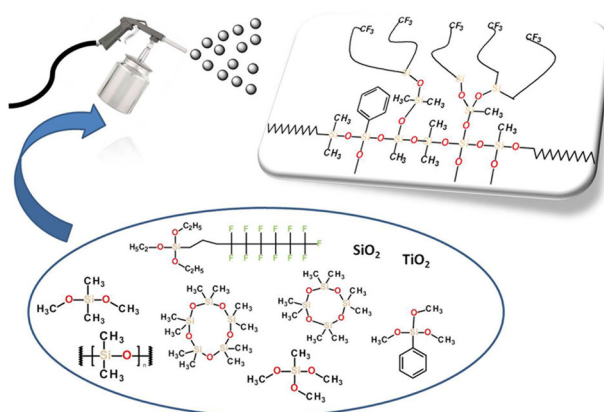
✉ Nilhan Kayaman-Apohan
napohan@marmara.edu.tr

[1] Department of Chemistry, Marmara University, 34722 Istanbul, Turkey

Highlights

- Sol–gel-based non-stick ceramic coatings were prepared.
- Coatings were applied onto aluminum substrates and were thermally cured.
- Ceramic coatings exhibited good adhesion.

1 Introduction

Since the mid-twentieth century, polytetrafluoroethylene (PTFE), which is better known by its brand name Teflon® (patented by DuPont), has been used to manufacture non-stick cookware [1]. Until now, the market for the non-stick cookware was dominated by PTFE-based products [2]. However, with the beginning of the twenty-first century, environmental concerns have been raised due to the release of a toxic pollutant, perfluorooctanoic acid (PFOA, an emulsifier used in the PTFE manufacturing), from over-heated pans. Even though PFOA is phased out and replaced by other surfactants such as ammonium 4,8-dioxa-3H-per-fluorononanoate (ADONA) [3], the use of PTFE in non-stick cookware lost its appeal. Therefore, many cookware manufacturers started to work on novel innovations and as a result, in recent years, several non-stick ceramic cookware products were commercialized as Teflon alternatives. These ceramic coatings are based on the well-known sol–gel chemistry.

The sol–gel method, which is based on the hydrolysis of metal alkoxides and their subsequent condensation reactions, is considered as a suitable procedure for preparing high purity and homogeneous films [4–7]. It is also the most preferred technique for fabricating organic–inorganic hybrid materials because it facilitates the control of the reaction conditions and it is an environmentally friendly system [8, 9]. A wide range of substrates, such as ceramics, polymer surfaces, metals, and glass, can be coated by the sol–gel technique. The resulting coatings have advantages including the ease of composition control, homogeneity, good adhesion, and the simple application procedures [10, 11]. Moreover, these ceramic coatings are eco-friendly. The non-stick properties of these ceramic coatings arise from the hydrophobic, low surface energy siloxane networks. Siloxanes are one of the most common groups in inorganic polymers and the siloxane bonds (Si–O) with organic side groups generate unique properties [12–14].

Even though, the patent literature on the preparation of non-stick ceramic coating compositions for cookware applications is rich [15–18], there are only a few scientific papers that directly deal with these ceramic cookware. For instance, Jeon and Kim were issued a patent for a non-stick ceramic coating composition developed from organic–inorganic hybrid materials, including colloidal silica, fluorinated silanes, and polydimethylsiloxane using the sol–gel process [15]. In another patent, Carre et al. reports a protective coating, which imparts non-stick, abrasion resistance and hydrophobic properties with an inorganic network from metal alkoxides and an organic network from silanes via a sol–gel process [16]. Baney et al. describes a new coating formulation composed of an acidic dispersion of colloidal silica in an alcohol–water mixture that generates a hard, abrasion-resistant coating [17]. Le Bris et al. discloses an invention related to a cooking item having a glassy coating with enhanced impact-resistance properties [18].

In this paper, we report the preparation of a sol–gel-derived coating material as a Teflon® alternative. The non-stick coating formulations include a SiO_x matrix that results from the condensation of the hydrolyzed alkoxysilanes and a colloidal silica sol that is very stable. Several properties of the coatings such as cross-cut adhesion, hardness, gloss, and contact angle (CA) were characterized in detail by scanning electron microscopy (SEM)/Energy Dispersive Spectroscopy(EDAX), X-ray photoelectron spectroscopy (XPS), Brunauer-Emmett-Teller (BET), and Barett-Joyner-Halenda (BJH) analyses. And also the roughness of the surface is quantitatively described by the root-mean-squared roughness (rms) which is the standard deviation in the height of the surface measured by the Atomic force microscopy (AFM) image.

2 Experimental

2.1 Materials

Colloidal silica (40%, Ludox HS–40, Sigma–Aldrich), methyltrimethoxysilane (Dynasylan® MTMS, EVONIK), dimethyldimethoxysilane (DMDMS, Sigma–Aldrich), tridecafluoro-1,1,2,2-tetrahydrooctyl triethoxysilane (FAS–Dynasylan® F8261, EVONIK), phenyltrimethoxysilane (PTMS–Dynasylan® 9165, EVONIK), octamethylcyclotetrasiloxane (D4, Sigma–Aldrich), decamethylcyclopentasiloxane (D5, Sigma–Aldrich), and silicon oil (food-grade methyl silicon oil, DOW CORNING® 200 Fluid, 1000cSt) were used as received. Acetic acid (Fluka, 99%, used as a catalyst) was used as received. Isopropyl alcohol (IPA) also was used as received. Deionized water of 18.2 MΩ cm

resistivity obtained from a milli Q-water purification system (Millipore, Anamed–Turkey) was used.

2.2 Characterization methods

The specific surface area and the average pore diameter of the powders were determined using the Quantachrome Autosorb Automated Gas Sorption System (Autosorb 1 for Windows 1.54). The isotherm data were used to calculate the specific area and the average pore diameter of the powders. Specific surface areas of the powders were determined using the Malvern Instruments Mastersizer 2000.

Coatings morphology was viewed under a scanning electron microscope (JEOL 6335F). The SEM analysis was operated at 20 kV accelerating voltage.

In order to determine the electronic state and chemical composition of the sol–gel coatings, XPS was performed by X-rays exposure under high vacuum.

The hydrophobic nature of the coating is evaluated by measuring the CA (θ) via a Kruss (Easy Drop DSA-2) tensiometer, equipped with a camera. Analyses were conducted at room temperature at a relative humidity of 50% in the laboratory by the sessile drop method. The liquid drop image captured by a video camera was transferred to a computer screen. The syringe was filled with distilled water and a drop (3–5 μl) was allowed to fall onto the substrate. Then the left and right CAs were measured for 10 s and subsequently averaged. Each measurement was repeated at least three times and the average was taken.

AFM images at tapping mode were obtained by using an Ambios-Quesant Q-Scope universal scanning probe microscope with an AFM attachment at room temperature.

The coating performance was measured with standard test methods as indicated; gloss (ASTMD-523-80), cross-cut (DIN 53151), pencil hardness (ASTM D-3363), and MEK rub test (ASTM D-5402). The reported values were the average of four measurements.

2.3 Preparation of surfaces

The pretreatment of surface is extremely important in improving the wettability and continuity and uniformity of the coatings. Additionally, it also influences the adhesion of the coating to the substrate, which indirectly affects the coating performance [19]. Scheme 1A and B shows the surface pretreatment method and reaction procedure. In this study, coatings were applied onto aluminum substrates. Oil and dirtiness were removed from the surface of aluminum substrate through chemical methods prior to the coating process, since any oil or grease can contaminate the blasting material and interfere with adhesion. They were cleaned using acetone and trichloroethylene (TCE) after the removal of the protective film. Following this cleaning and then drying, sand blasting process was carried out in order to improve the adhesion strength of the coating material to the aluminum surface. If the surface is too smooth, it can negatively affect both adhesion and mechanical performance. After surface roughness was completed, the surface was cleaned again. After the entire process was completed,

Scheme 1 (a) Surface pretreatment of the aluminum substates and (b) spray coating of the treated aluminium surfaces with the non-stick fluorinated ceramic coating
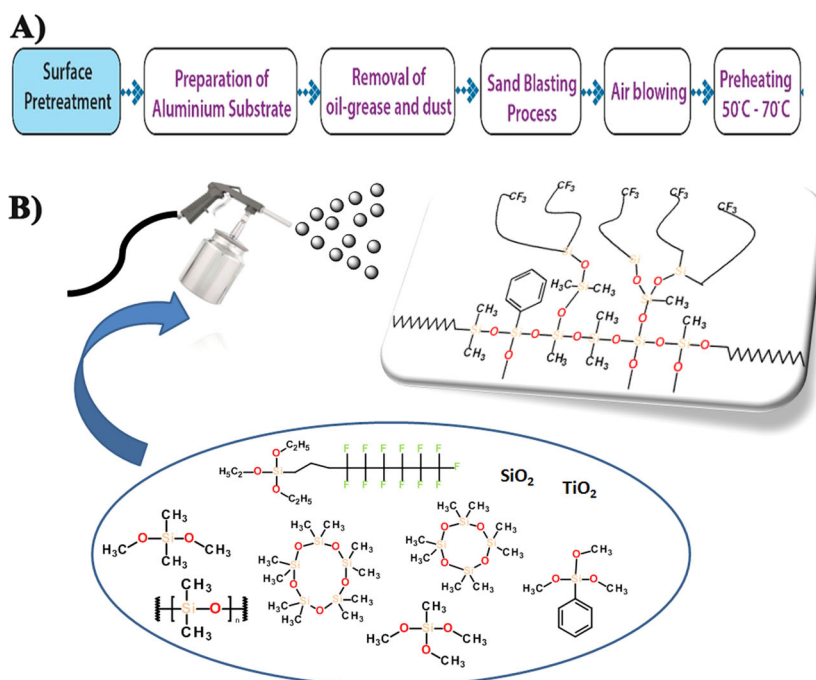
the base and topcoat solutions were applied on the surfaces through spraying method.

2.4 Preparation of the silane precursor of base coat (M3)

The component A for base coat was prepared by using silica sol, Ti paste (60% TiO_2 in IPA), IPA, and silicone oil as follows: colloidal silica (40 wt.%, 52.0 g), Ti paste (60 wt. %, 31.2 g), IPA (17.6 g, 0.293 mol), and silicone oil (3.2 g) were charged into a bottle. The mixture was magnetically stirred at room temperature for about 2 h. A white suspension was obtained.

The precursor sol component B for base coat was prepared by using MTMS (24.0 g, 0.176 mol), DMDMS (16.0 g, 0.133 mol), PTMS (2.4 g, 0.0121 mol), and FAS (4.0 g, 0.0078 mol) as the precursor alkoxides. Then 9.6 g of D4:D5 (80:20 weight ratio) was added to this mixture. The mixture was magnetically stirred at room temperature for about 1 h. A clear solution was obtained. After the component A and B solutions were prepared separately, 50.0 g of component A and 26.9 g of component B were mixed. Acetic acid (used as a catalyst) was added to the mixture to adjust the pH to 2–3.

2.5 Preparation of the silane precursor of topcoat (M3)

The component A for the topcoat was prepared by using silica sol, IPA, and silicone oil as follows: colloidal silica (40 wt.%, 72.8 g), IPA (12.0 g, 0.2 mol), and silicone oil (3.2 g) were charged into a bottle. The mixture was magnetically stirred at ambient temperature for about 2 h.

The precursor sol component B for the topcoat was prepared by using MTMS (39.2 g, 0.288 mol), DMDMS (16.8 g, 0.140 mol), PTMS (2.4 g, 0.0121 mol), and FAS (4.0 g, 0.0078 mol) as the precursor alkoxides. Then D4:D5 (9.6 g, 0.0288 mol) was added to this mixture. A transparent solution was obtained after the mixture was magnetically stirred at ambient temperature for about 1 h. Then 50.0 g of component A and 40.9 g of component B were mixed. A catalytic amount of acetic acid was added to the final mixture.

2.6 Application of the coating mixture (M3)

After surface preparation, the base and the topcoats were applied on the surface of preheated aluminum substrates (65 °C) by using a pneumatic spray. In order to obtain the best spray pattern, many trials were conducted on the aluminum substrates. As known, spraying conditions and spray equipment are very important for studies like these because they significantly affect the coating performance. For instance, the usage of large nozzle size can result in the large size of droplets, which could affect the uniformity and texture of the coating layer. The optimum settings were as follow: spraying distance of 60 cm, nozzle diameter of 1.0 mm, and air pressure of 50 psi. The preheating is an important step, else the sol–gel coating could sag. In this step, IR thermometer was used to measure the right temperature. The milky suspensions were ultrasonicated to remove air bubbles prior to spraying process. After air bubble removal, the primer solution was deposited on roughened aluminum substrates with spray-coating at 65 °C for 60 s. The wet film thickness of the base coat is between 40 and 50 microns. Then the topcoat is sprayed over the base coat prior to its drying for 30 s. The coated samples were oven dried at 260 °C (Memmert) for 1 h to obtain cross-linked sol–gel network. During the heat treatment, the condensation reactions of the alkoxy (OR) and the hydroxyl (OH) groups ftook place for the formation of the sol–gel based network. The dry coating thickness was found to be between 40 and 60 microns.

Table 1 shows the base and topcoat compositions of non-stick coating formulations. Moreover, the quality of the coating can be seen in the movie (Online Resource 1)

3 Results and discussion

In this study, a two-layer coating system which consists of a base and a top layer was developed. The base and top-coat formulations were prepared separately. Both coating compositions have two individual components, A and B. The component A is composed of colloidal SiO_2, titania paste (Ti paste), IPA, and silicone oil. Component B is a mixture of organoalkoxysilane compounds (MTMS, DMDMS, FAS), D4, D5, and PTMS. Since water and alkoxysilanes are immiscible, the compatibility was improved by the addition of IPA as solvent. The base coat is the first layer that is applied to the aluminum surface. The topcoat is the second layer, which is applied over the first layer (the base coat). The base coat is the sol–gel material which binds to the surface of the substrate mechanically and to the topcoat chemically. It improves the adhesion and imparts color. The two-layer system was designed to obtain sufficient mechanical properties. The difference between the topcoat and the base coat is the use of the titania paste and the amount of materials. Table 2 shows the chemical structure of all the components and their role in the formulations.

In this study, the main matrix is composed of a network of silica formed by the condensation of colloidal silica sol and MTMS, DMDMS, FAS, and PTMS mixture by the sol–gel process. All components (colloidal silica sol and organoalkoxysilane mixture, MTMS–DMDMS–FAS–PTMS) can

Table 1 The base and topcoat compositions of coating formulations

The base coat compositions

Sample codes	Component A (65%, wt./wt.)				Component B (35%, wt./wt.)			
	Colloidal silica (40 (wt.%)) (wt.%)	IPA (wt. %)	Titania paste (60 (wt.%)) (wt.%)	Silicone oil (wt.%)	MTMS:DMDMS 60:40 (wt.%)	D_4:D_5 (wt.%)	FAS (wt. %)	PTMS (wt. %)
M1	32.5	12	19.5	1	27.5	6	–	1.5
M2	32.5	15	17.5	–	34.5	–	–	0.5
M3	32.5	11	19.5	2	25	6	2.5	1.5
The topcoat compositions								
Sample Codes	Component A (55%, wt./wt.)				Component B (45%, wt./wt.)			
	Colloidal silica (40 (wt.%)) (wt.%)	IPA (wt. %)	Titania paste (60 (wt.%)) (wt.%)	Silicone oil (wt.%)	MTMS:DMDMS 70:30 (wt.%)	D_4:D_5 (wt.%)	FAS (wt. %)	PTMS (wt. %)
M1	45.5	8.5	–	1	37.5	6	–	1.5
M2	42.5	12.5	–	–	44.5	–	–	0.5
M3	45.5	7.5	–	2	35	6	2.5	1.5

make strong chemical bond by condensation reaction. FAS was only used in M3 formulation. It increases crosslinking degree of the coating in the network. It also helps hydrophobicity of coating. The alkoxy groups are hydrolyzed by water in the presence of an organic acid catalyst (acetic acid) and then condensation reaction proceeds under mild conditions as can be seen from Scheme 2. Hydrolysis reactions in the sol–gel produces the reactive groups which will form polymer links. Then once silanol groups (Si–OH) form, they condense through two different reactions to form silicon–oxygen–silicon (Si–O–Si) bridges [20]. The organic and inorganic constituents of the new hybrid material can interpenetrate each other in microscopic level from a few micrometers to a few nanometers. Finally, a three-dimensional silica network is formed when sprayed on the surface of the substrate.

3.1 BET and BJH plots of the coatings (surface area and porosimetry)

The adsorption–desorption isotherms of nitrogen (N_2) were carried out to examine the morphological and physical properties of the base and topcoat for M3.
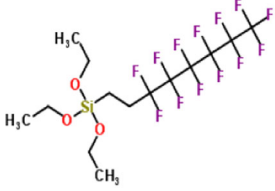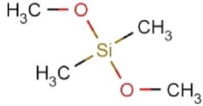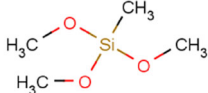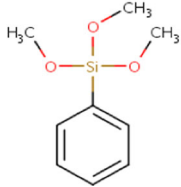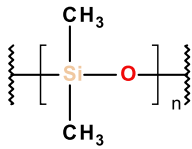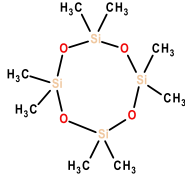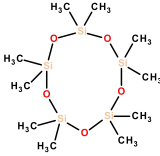
Figure 1a, b presents the nitrogen (N_2) adsorption (red)/ desorption (blue) isotherms measured at 77 K for the base and topcoats, respectively. From this measurement, the structural parameters including specific surface area, pore volume, and average pore diameter of base and topcoat of M3 were derived as shown in Table 3. From Fig. 1, it seems that the coat exhibits Type II isotherm according to IUPAC classification [21]. This type is related to multilayer physical adsorption and describes strong interactions between the adsorbate and adsorbent [22, 23].

The BET surface areas, specific surface areas, average pore diameter, and average pore volume of the base and topcoat calculated by BET and BJH methods are listed in Table 3. As the results are presented in Table 3, the base and topcoat coatings have surface area values over of 100 m^2/g. This result can be attributed to a uniform and smooth surface formation. According to the IUPAC classification of the isotherms, the pores with a diameter not exceeding 2 nm are defined as micropores and the ones with a diameter between 2 and 50 nm are named as mesopores [24]. In addition, micropores can be categorized as ultramicropores (width <0.5 nm) and supermicropores (width from 1–2 nm) [25]. These values are important since the quality of non-stick coatings is directly affected. The results clearly showed that the base and topcoat of M3 have the average pore diameter of 2.726 nm (mesopore) and 1.807 nm (supermicropore), respectively. These findings indicate that the particles clump and stick together with an increase in the colloidal silica content and the size of the particles slightly decreases, which leads to an increase in the surface area.

The insets of Fig. 1 show the pore size distributions of the component A of the base and topcoats. The differential pore volume is plotted against pore radius (size) from the desorption branches of the N_2 adsorption–desorption isotherms according to BJH model [26]. This method is based on the assumption that the initial relative pressure is close to unity and all the pores are filled with adsorbate liquid. The BJH adsorption surface areas of pores for base and topcoats were calculated as 126.92 and 170.08 m^2/g, respectively. According to these results, the topcoat possesses micropore structure with narrow pore size distribution. The topcoat has a large number of pores compared to base coat and the pore size is smaller than base coat. BET analysis revealed that the surface area of the coatings decreased with an increase in pore size of the coatings.

Table 2 Organoalkoxysilane compounds and their structure and acronyms

Material	Functionality	Role in the coating	Structure
FAS (tridecafluoro-1,1,2,2-tetrahydrooctyl triethoxysilane-(Dynasylan® F8261)	Trifunctional – fluoroalkyl	Hydrophobicity Crosslinking	
DMDMS (Dimethyl dimethoxysilane)	Bifunctional – alkyl	Takes place in siloxane network, Decreases crosslinking and thus cracking during thermal curing	
MTMS (Methyl trimethoxysilane)	Trifunctional – alkyl	Forms siloxane network	
PTMS (Phenyltrimethoxysilane -Dynasylan® 9165)	Trifunctional – aryl	Thermal stability Takes place in crosslinking Hydrophobicity	
Silicone oil (1000 cSt)	-	Prevents craking Thermal stability	
Titania Paste	-	Pigment Increases adhesion Takes place in crosslinking	TiO_2
Colloidal Silica	-	Takes place in crosslinking Increases durability and mechanical properties	SiO_2
D4 (Octamethyl cyclotetrasiloxane)	-	Increases molecular weight Adjusts mechanical propoerties	
D5 (Decamethyl cyclopentasiloxane)	-	Increases molecular weight Adjusts mechanical propoerties	

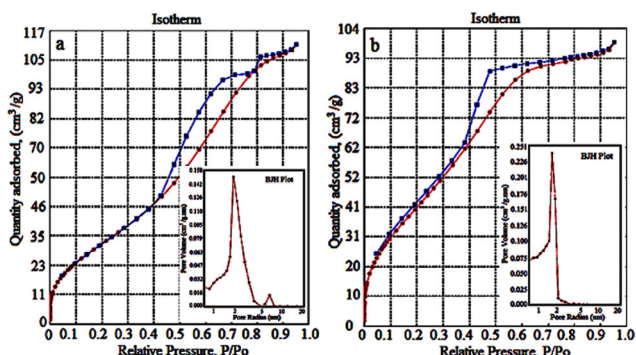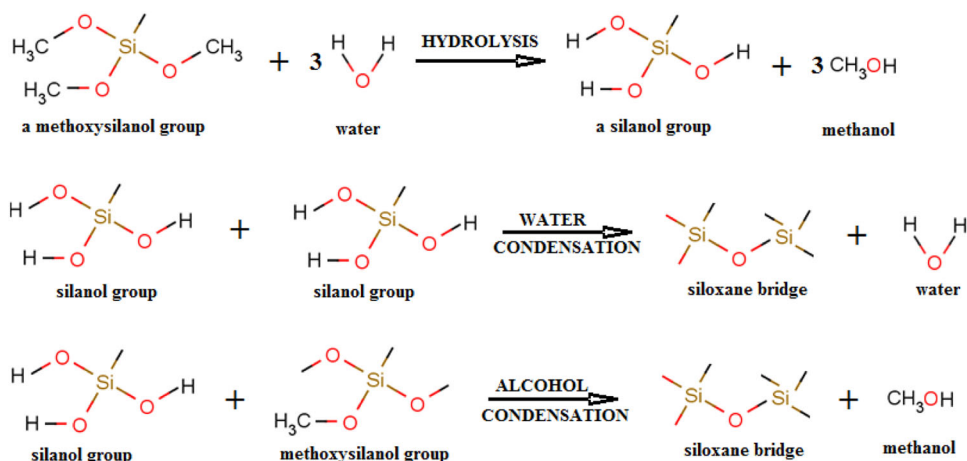**Scheme 2** The sol-gel process

Fig. 1 N2 adsorption-desorption isotherms and pore size distribution of the (**a**) base and (**b**) top coat (M3)

3.2 Morphology

The elements distribution in the cross-sections of the sol–gel-coated aluminum substrate was examined by SEM/EDAX analysis. SEM/EDAX spectra of the base and top-coat are given in Fig. 2a, b, respectively. The analysis results clearly show that the smooth and homogenous part of the micrographs mainly contains O and Si elements coming from sol–gel formulation of topcoat. However, the patchwork regions are titanium (Ti)-rich areas within the sol–gel-based base coat. The topographic morphology of the sol–gel coatings were investigated by AFM. Two and three-dimensional topographic AFM images of the sand-blasted and coated Al substrates are presented in Fig. 3. Clearly, the surface of the blasted specimen is rough with numerous ''peaks'' and ''valleys''. This is due to the high surface roughness resulted from the sandblasting process. Before coating, the surface roughness of aluminum substrate plays a vital role for surface chemistry and effect on the performance of coatings. After sanding process, a more porous/valleys structure increases the coating solution penetration, and as a result, it promotes the adhesion of the non-stick coating on the aluminum substrate. The average

heights of the sandblasted substrate, $M1$, $M2$, and $M3$ were found as 616.2, 178.2, 30.10, and 344 nm respectively, while the root mean square deviation results (rms) were determined as 233.4, 54.21, 6.945, and 44 nm for the same series of materials.

3.3 XPS analysis

XPS analysis was used to determine the electronic state and chemical composition of the coatings [27]. In addition, the quantitative results with the atomic ratios are given. X-ray photoelectron spectra in Fig. 4 show the comparison between fluorine-based coating (M3) and the non-fluorinated coatings (M1 and M2). In addition, the atomic ratios are summarized in the insets of Fig 3. The curve corresponding to coated samples shows relative intensities of silicone, oxygen, carbon, and fluorine (Si, O, C, and F). The Kα signal of Si2p spectra was observed at around 102.55, 102.93, and 102.90 eV, for samples M1, M2, and M3, respectively. The signal of oxygen O1s was observed at around 532.53, 532.49, and 532.56 eV, for samples M1, M2, and M3, respectively. The signal of carbon C1s is also observed at around 285.00 eV for all of the coatings. A weak peak due to F1s was seen at 689.35 eV for M3 sample, whereas, no signals were observed in the case of non-fluorinated coating samples (M1 and M2). According to the XPS survey spectrum, the atomic ratio of Si, O, C, and F elements on the surface of M3 is as follows: $N_{Si}/N_C/N_O/N_F = 28.4/38.9/29.6/3.1$ (atomic ratio).

3.4 FTIR analysis

The FTIR spectra of the coatings are presented in Fig 5. As can be seen from this figure, all coatings displayed similar spectra. The bands between 3000 and 2800 cm^{-1} are due to the -CH$_2$ and -CH$_3$ groups. The peaks at around 995 and 1087 cm^{-1} correspond to the –Si–O–Si– linkages, but at the

Table 3 The specific surface area, surface area, average pore diameter, and average pore volume of the base and topcoat (M3)

| Component	Sample weight[a] (g)	Concentration[b] (% volume)	Specific surface area[b] (m²/g)	Surface area[a] (m²/g)	Average pore diameter[a] (nm)	Average pore volume[a] (cm³/g)
Base coat	0.0828	0.0085	4.05	126.92	2.726	0.1730
Topcoat	0.0419	0.0204	0.545	170.08	1.807	0.1537

[a]Determined by BET and BJH analysis

[b]Determined by particle size analyzer
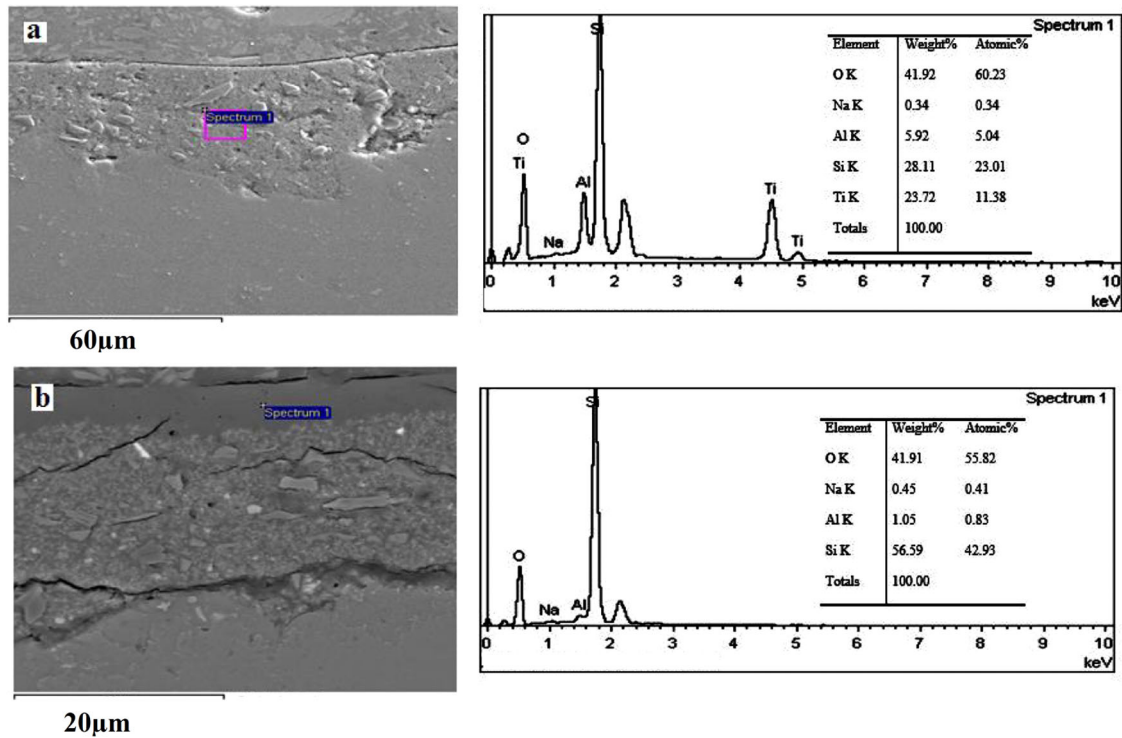
Fig. 2 SEM image and EDAX of the cross-section of the sprayed coating on aluminum substrate **a** Basecoat (M3), **b** Top coat (M3)
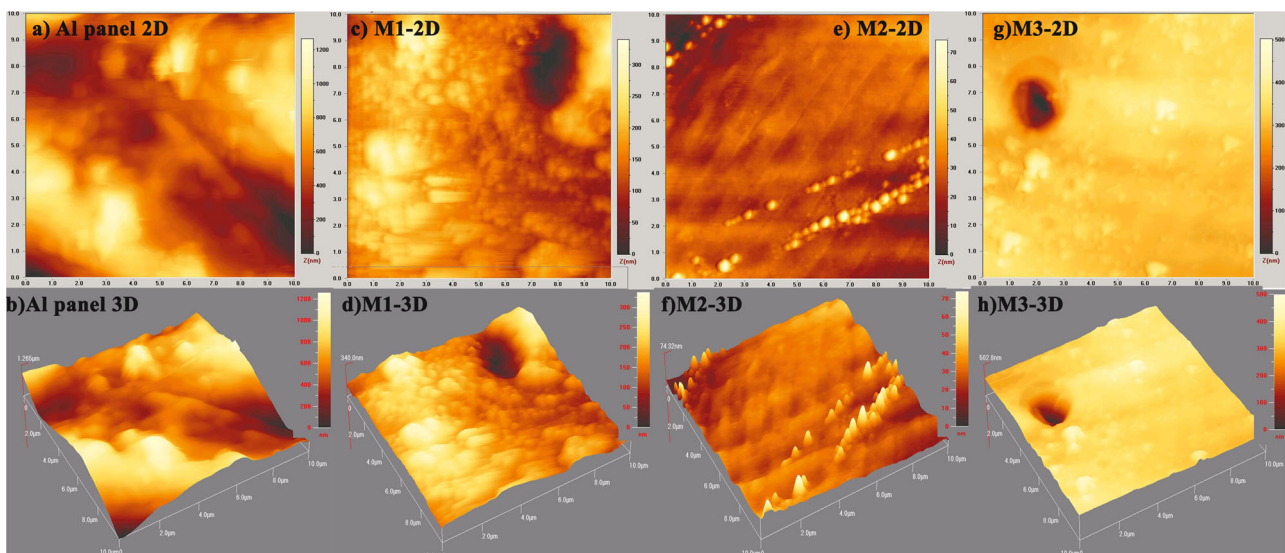
Fig. 3 AFM images of sandblasted aluminum panels, M1, M2 and M3

Fig. 4 XPS spectra of the top surface of **a** M1, **b** M2 and **c** M3
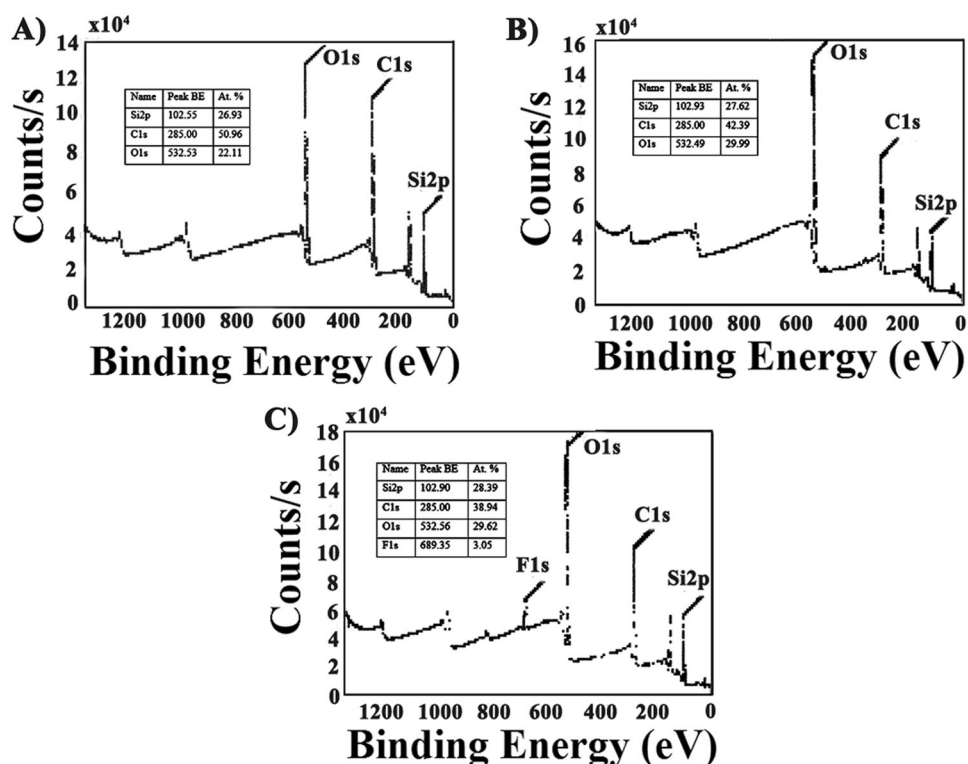
Fig. 5 FTIR spectra of M1, M2 and M3
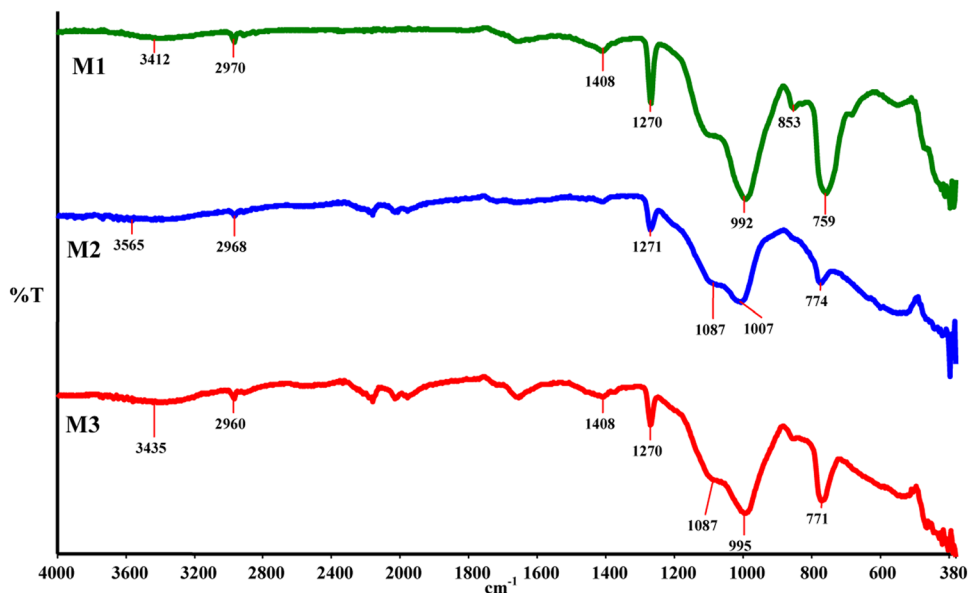
same time the band 1087 cm^{-1} can be related to the presence of –Si–O–C–, –Si–C– bonds [28]. We were not able to observe the peaks related to carbon-fluorine absorptions and this situation can be ascribed to the low level of FAS in the coatings. The –OH stretching vibrations were observed in low intensity at around 3500–3400 cm^{-1}, which indicates that due to the high crosslinking density of the sol–gel coatings, the amount of the residual hydroxyl groups is low. The bands at 1270, 853, and 774 cm^{-1} which were due to

the presence of strong chemical bonds as Si–O–CH$_3$ (CH$_3$ rocking) and Si–C in the obtained coatings were observed [28]. Finally, it can be concluded that in the synthesized non-stick coatings, strong chemical covalent bonds existed.

3.5 CA measurements

CAs are very susceptible to the surface composition variations [29]. There is a direct correlation between CA and

Table 4 Physical and mechanical properties of sol–gel coatings

	Gloss			MEK rubbing test	Pencil hardness	Cross-cut	Contact angle (°)	Boiling water test
	20°	60°	85°					
M1	4	28	55	500+	5H	5B	97	No paint delamination
M2	4	22	46	300	5H	1B	85	Some paint delamination
M3	11	47	68	500+	6H	5B	106	No paint delamination

Fig. 6 Cross-cut results of sol-gel-coated Al substrates
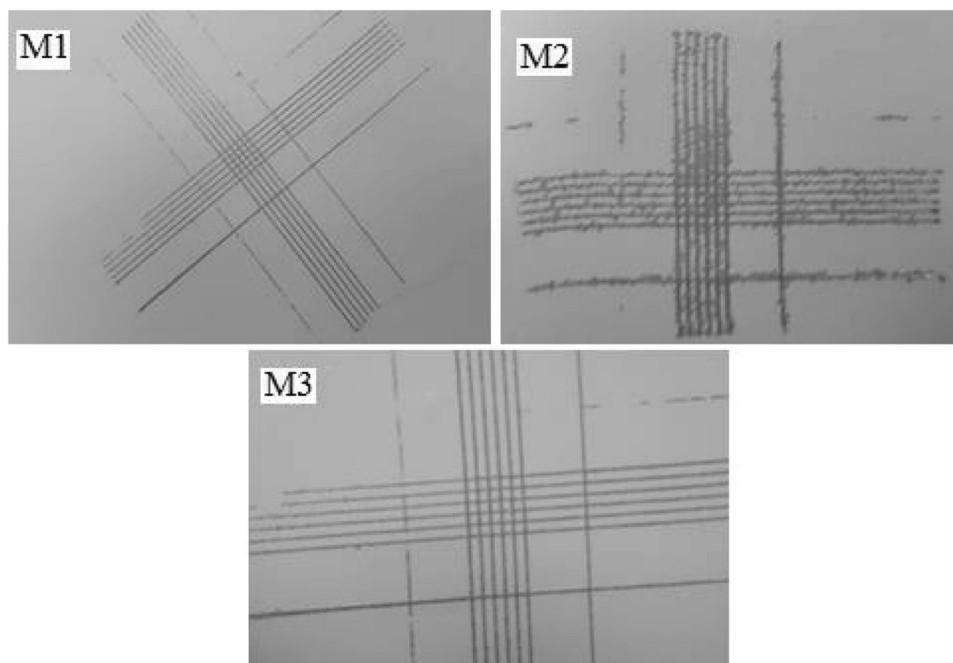
hydrophobicity. Each CA value is given in Table 4, represents an average of five readings to minimize the experimental error. As expected, M3 sample shows better hydrophobicity than M1 and M2 samples due to its fluorine content and had an average CA of about 106°. In addition, M3 coating also contains PTMS, which exhibits excellent hydrophobicity when used with FAS together. When M1 and M2 were compared, it is clearly observable that the addition of higher amount of PTMS increases the hydrophobicity. This could be attributed to the aryl and silane structural influence. Additionally, it is well known that siloxane-containing networks possess very low surface energy [30]. Finally, the samples M1 and M2 had CAs of 97° and 85°, respectively.

3.6 Physical and mechanical properties of sol–gel coatings

The results of the physical and mechanical performance tests of the coating materials such as gloss, solvent resistance, pencil hardness, cross-cut, CA, boiling water test are also collected in Table 4.

The degree of crosslinking and chain flexibility of the sol–gel coating plays a major role on the hardness [31]. Pencil hardness properties of sol–gel coating was determined using pencil hardness tester (BYK Gardner) with a calibrated set of drawing leads ranging from 6B (the softest) to 6H (the hardest). It is known that the hardness of the coatings depends on the chemical structure and the cross-linking density. As it can be seen from Table 4, the pencil hardness of all the coatings is greater than 4H and it was found as 6H for M3.

As it can be seen in Fig. 6, cross-cut properties of sol–gel coatings were found 5B except for sample M2. This result means the edges of cuts are completely smooth and none of the squares of the lattice are detached. However, M2 coating has flaked along the edges of the cuts and almost whole squares have detached. The cross-cut adhesion result was found as 1B for M2. This result was attributed to the absence of the silicone oil in M2. The presence of silicone oil prevents cracks and increases the adhesion. The long linear siloxane units in silicone oil increase the flexibility of the coatings and release the stress formed during the crosslinking reactions that occur between two–three

functional small alkoxysilane compounds. Moreover, it also helps to reduce the surface tension of the liquid precursor. Thus, during the drying process, the wetting of the aluminum substrate by the coating material is eased. Hence the adhesion performance of the coating is improved.

As it can be seen from the results, both the adhesion and surface hardness properties of the coatings are influenced by the solid content, composition, surface porosity, and degree of crosslinking. The type of alkoxysilane used or organic content in the final siloxane/silica network can influence the mechanical strength and the adhesion properties. Namely, this study reports the synthesis via sol–gel method of silica and organic chain networks with a mixture of MTMS and DMDMS in higher proportions compared to FAS and PTMS. When M1, M2, and M3 coatings are compared, it can be seen that they contain different molar proportions of MTMS:DMDMS.

The solvent resistance of the sol–gel coatings was examined by performing the MEK rubbing test. The coatings M1 and M3 were unaffected after 500 double rubs. This result indicates that these sol–gel-based coatings are highly crosslinked and well adhered. Besides this, the solvent resistance of the films was also examined by immersing the coating samples in various solvents (37% HCl, 65% NaOH, acetone, xylene) for 24-h time period. The general physical appearance of the coatings was perfect and no cracks or pinholes were observed.

It is known that coating's gloss is a complex phenomenon resulting from the interaction between the surface of the coating and light [32, 33]. Specifically, the gloss is affected strongly by surface roughness in the clear coating system [34]. In this study, the measurements showed that the presence of flourine in the sol–gel coating, M3, increases the gloss value when compared to the other samples (M1 and M2). The changes in gloss between M1 and M2 can be explained by the presence of different weight fractions of PTMS and $D_4:D_5$. This may be attributed to more effective crosslinking, which resulted in more uniform, homogenous, and smooth surface.

Adhesion strength of the coated samples was also characterized by boiling them in water for 1 h. Water molecules that penetrate through the sol–gel coating to the surface can cause blistering and loss of adhesion [35]. Hence, this test examines a coating's ability to adequately protect the surface in immersion conditions. For samples M1 and M3, the obtained data clearly showed that these formulations have very good adhesion properties. No cracks, peeling, or stains were observed for these two samples.

Finally, egg test performance of the sol–gel-based coatings was compared (Fig. 7). Egg test is a common standard test to evaluate the non-stick properties and stain resistance of the cookware. In this test, an egg is broken onto the
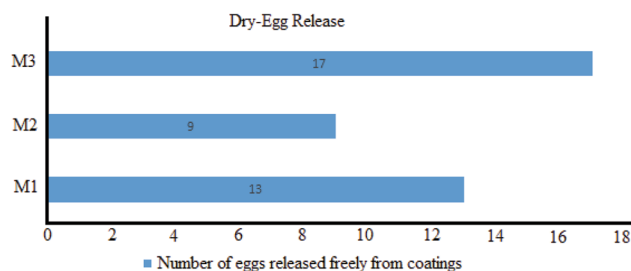

Fig. 7 Comparison of number of eggs released from coatings

preheated pan (175 °C) and cooked for 2.5 min. Then it is removed from the pan using a spatula. The test is repeated until the ease of lifting the eggs is lost. The egg release test results of M1, M2, and M3 were found as 13, 9, and 17, respectively. Results clearly showed that sol–gel-based coatings tend to have good release values when compared to some commercial products [36]. Especially, the fluorine-containing formulation, M3, shows the best dry-egg release. These findings clearly show that the sol–gel coatings were successfully applied on the aluminum substrate and could possibly be used in cooking materials with further improvement.

4 Conclusion

Non-stick fluorine-containing ceramic coatings were prepared by the sol–gel technique for aluminum substrates as an alternative to Teflon-based cookware. Different formulations were prepared to test the effect of silicone oil and fluorine. Formulations were applied onto preheated aluminum substrates and then cured at 260 °C for 1 h. Surface properties of the coatings were investigated by AFM, SEM/EDAX, and XPS analyses. The chemical structure of the coatings was characterized by FTIR measurements. Almost all coatings displayed promising properties and can be used as cookware materials. Boiling water and dry-egg releasing tests were evaluated successfully. The sol–gel coating with the highest amount of fluorine displayed the best performance. Nevertheless, some of the long-term properties of the coatings were found to be limited for cooking material applications, and therefore more tests will be done in future studies and new formulations will be designed to improve the performance of these coatings.

Compliance with ethical standards

Conflict of interest The authors declare that they have no conflict of interest.

References

1. Groll WA (2009) Method of making non-stick cookware. US Patent 7488515 B2
2. Rossi S, Gai G, De Benedetto R (2014) Mater Des 53:782–790
3. Schlummer M, Sölch C, Meisel T, Still M, Gruber L, Wolz G (2015) Chemosphere 129:46–53
4. Tari O, Aronne A, Addonizio ML, Daliento S, Fanelli E, Pernice P (2012) Sol Energy Mater Sol Cells 105:179–186
5. Znaidi L, Touam T, Vrel D, Souded N, Yahia SB, Brinza O, Fischer A, Boudrioua A (2013) Coatings 3:126–139
6. Oh EO, Chakrabarti K, Jung HY, Whang CM (2002) Mater Sci Eng B 90:60–66
7. Haas KH, Amberg-Schwab S, Rose C (1999) Thin Solid Films 351:198–203
8. Wang D, Bierwagen GP (2009) Progress Org Coat 64:327–338
9. Xiao X, Hao C (2010) Colloids Surf A Physicochem Eng Asp 359:8–87
10. Yu JG, Yu JC, Ho WK, Jiang ZT (2002) New J Chem 26:607–613
11. Jing C, Xu X, Hou J (2007) J Sol-Gel Sci Technol 43:321–327
12. Yilgor I, McGrath JE (1988) Adv Polym Sci 86:1–86
13. Kraxner P, Boogh L, Lejenue A (2000) The role of silanes in filled and crosslinked polymers, Organosilicon Chemistry Vol IV: from molecules to materials. Wiley-VCH, New York, p 562–572
14. Gates DP, (2002) Inorganic and organic polymers Annu Rep Prog Chem A 98:479–492
15. Jeon BY, Kim SM (2007) Non-stick ceramic coating composition and process. US Patent 20070218297 A1
16. Carre A, Prassas M, Waku-Nsimba J (2000) Coating for imparting non-stick, abrasion resistant and non-wetting properties to inorganic articles. US Patent 6054522A
17. Baney RH, Chi FK (1981) Pigment-free coatings with improved resistance to weathering. US Patent 4275118A
18. Le Bris S, Dubanchet A, Perillon JL (2011) Cooking item comprising a non-stick coating with improved properties of adhesion to the substrate. US Patent 20110180546 A1
19. Kumar N, Jyothirmayi A, Soma Raju KRC, Subasri R (2012) Ceram Int 38:6565–6572
20. Kang S, Hong S, Choe CR, Park M, Rim S, Kim J (2001) Polymer 42:879–887
21. Rouquerol J, Avnir D, Everett DH, Fairbridge C, Haynes M, Pernicone N, Ramsay JDF, Sing KSW, Unger KK (1994) Stud Surf Sci Catal 87:1–9
22. Hassani A, Kıranşan M, Soltani RDC, Khataee A, Karaca S (2015) Turk J Chem 39:734–749
23. Budnyak TM, Pylypchuk IV, Tertykh VA, Yanovska ES, Kolodynska D (2015) Nanoscale Res Lett 87:1–10
24. Al-Othman ZZ, (2012) A review: fundamental aspects of silicate mesoporous materials Materials 5:2874–2902. https://doi.org/10.3390/ma5122874
25. Wang X, Li D, Li W, Peng J, Xia H, Zhang L, Guo S, Chen G (2013) Bioresources 8:6184–6195
26. Barett EP, Joyner LG, Halenda PP (1951) J Am Chem Soc 73:373–380
27. Turner RH, Boerio FJ (2002) J Adhes 78:465–493
28. Samuneva B, Kabaivanova L, Chernev G, Djambaski P, Kaschieva E, Emanuilova E, Salvado IMM, Fernandes MHV, Wu A (2008) J Sol-Gel Sci Technol 48:73–79
29. Karataş S, Hoşgör Z, Kayaman-Apohan N, Güngör A (2009) Progress Org Coat 65:49–55
30. Marra KG, Chapman TM, Orban JM (1996) Macromolecules 29:7553–7558
31. Karataş S, Hoşgör Z, Menceloğlu Y, Kayaman-Apohan N, Güngör A (2006) J Appl Polym Sci 102:1906–1914
32. Mülazim Y, Kahraman MV, Kayaman-Apohan N (2011) J Sol-Gel Sci Technol 59:613–620
33. Zong Z, He J, Soucek MD (2005) Progress Org Coat 53:83–90
34. Wicks ZW, Jones FN, Pappas SP (1994) Inorganic coatings: science and technology, vol 1. Wiley, NY
35. Tator KB, KTA-Tator Inc (2015) ASM handbook, volume 5B. Protective organic coatings, coating deterioration. ASM International, Ohio, USA
36. Fusion—PFOA and PTFE free sol-gel flier. https://www.whitfordww.com/download-literature.html. Accessed 06 Apr 2018.